Optica Applicata, Vol. XXIV, No. 1–2, 1994

GRIN lenses manufactured by diffusing index modifying cations into a sol-gel matrix

N. KOONE, Y. SHAO, T. W. ZERDA

Physics Department, Texas Christian University, Fort Worth, TX 76129, USA.

Diffusion coefficients of selected solvents (acetone, acetonitrile, water, chloroform, cyclohexane, toluene) in porous sol-gel glass were measured using radioactive tracer diffusion, diaphragm method, UV-VIS and IR spectroscopies. It was shown that translational motion inside the pores is greatly hindered by geometrical restrictions. Polar molecules diffuse faster than innert molecules. The results for cyclohexane were compared with molecular dynamics computer simulations and the tortuosity factor was evaluated. Water and acetone neodymium nitrate solutions were used to impregnante porous sol-gel glass. Diffusion coefficient for Nd^{3+} in aqueous solutions was slower than in acetone solutions. Concentration gradients inside the materials were produced by controlling the time the sample was exposed to the solution. To maintain the concentration profile during the drying stage of the process, the mobility of the solvent must be faster than that of the solute. When the sample was sintered neodymium was incorporated into the glass network. It was shown that both diverging and converging GRIN lenses can be produced.

1. Introduction

A flat GRIN glass having a continuous variation of the index of refraction can be used as a lens. The so-called radial GRIN lens has cylindrical shape and its index of refraction changes as

$$n(r) = n_0[1-(gr)^2] \tag{1}$$

where: n_0 – refractive index at the centre axis, r – radial distance from the symmetry axis, g – constant. The techniques used include ion exchange, chemical vapour deposition, double ion exchange, sol-gel processing, and others. Using the ion exchange proces [1], it is possible to obtain material having large change in n between the centre and the perimeter, but only samples of small diameters can be obtained. The double exchange process [2] allows manufacturing large lenses, but only of small variation of the index of refraction. In principle, using the sol-gel process, it is possible to fabricate lenses of large radii and large Δn. Growing interest in production of sol-gel glass of controlled concentration of metal cations results from pioneering work of YAMANE [3], CALDWELL *et al.* [4], KONISHI [5], and HENCH *et al.* [6]. Two alternative pathways are used in making gradient index glass. Different metal alkoxides can be mixed together during the wet stage of the sol-gel process, and after gelation, the index modifying ions are leached from the gel. However, problems associated with drying and firing of the gels limit this method only to small samples, about 3 mm in diameter. In this paper, we report the

first attempt to produce a GRIN lens by doping a sol-gel glass sample with a desired concentration profile of a metal cation, and thus continuously modify the index of refraction as a function of the sample radius.

During the past decade the formation of monolithic glass bodies via the sol-gel technique has been extensively studied, because of the many advantages this technique has over conventional glass melting. The sol-gel process begins with the hydrolysis of metal alkoxides, usually silicon tetramethylalkoxide or tetraethylalkoxide, followed by polymerization reaction [7]. The sol undergoes transition to a wet gel which with time elapsed becomes a solid, 3-dimensional porous aggregate of very small spherical particles. These reactions are usually done at the room temperature. In order to obtain a monolithic glass, wet sol must be dried to remove liquids present in the pores between the particles. Next, the 3-dimensional network of loosely connected SiO_2 bonds can be converted into a stable monolith by sintering at a temperature well below the melting temperature of glass.

Monolithic glasses obtained using the sol-gel processing have porosity that can be easily controlled. In addition, unique compositions of sol-gel glass are very difficult or even impossible to obtain using traditional melting technology. Another important advantage of the process is homogeneity of the product which is basically free of contamination.

Sol-gel glass produced by the method developed by Hench and West exhibits pore diameters that do not change during the heat treatment [8], [9]. In the temperature range from 400° C to 950° C, the pore sizes remain the same, only their number is reduced with increased temperature. The pores are interconnected and can be easily impregnated with liquids, gases and liquid solutions of solid materials. Impregnated glasses may also find applications in fast switching devices, such as Kerr cell [10], dye lasers [11], pH sensors [12], chemical [13] and biochemical [14] sensors, nonlinear optical devices [15], [16], and others.

In order to introduce a solid dopant into the pores, it must be first melted or dissolved in a liquid carrier. Experimentally it is simpler to use a latter method because the doping can be conducted at a room temperature and no external pressure is required. It is obvious that in order to understand transport properties of the dopant we must first understand the bahaviour of the carrier. Therefore, in this paper we will first discuss the motion of the solvent molecules in the pores. Experimental data for cyclohexane will be compared with computer simulation results. Next, we will concentrate on the discussion of the diffusion of neodymium cations in the pores of various sizes, and we will explore possibilities of producing flat gradient index, GRIN lenses by doping porous sol-gel glass with neodymium.

2. Experimental

2.1. Sol-gel process

The preparation of porous glass samples was carried out by acid catalysed hydrolysis of tetramethoxysilane (TMOS). Hydrolysis

$$Si(OCH_3)_4 + 4H_2O \rightarrow Si(OH)_4 + 4CH_3OH \quad (2)$$

and subsequent polymerization through water or alkohol producing reactions:

$$Si(OH)_4 + Si(OH)_4 \rightarrow =Si-O-Si= + H_2O, \quad (3)$$
$$Si(OH)_4 + Si(OCH_3)_4 \rightarrow =Si-O-Si= + CH_3OH \quad (4)$$

are followed by aging, drying and firing processes [16]–[19]. Gels densified at low temperature break when in contact with liquids, and to avoid this problem the samples were stabilized at 800° C. All the samples used in this study were optically transparent monoliths in the form of a cylinder 6 mm in diameter and lengths varying from 20 mm to 80 mm. The pore diameters, surafce area, and pore volume were measured using the BET technique. Samples had relatively narrow pore size distributions, an example is shown in Fig. 1. By changing the pH of water and altering the drying schedule, we produced samples of distinctly different pore diameters, ranging from 2.0 nm to 22 nm. After preparation samples were immediately stored under nitrogen. Prior to use, the samples were dried under vacuum at 200° C for about 3 hours. Evacuated samples to vacuum better than 0.1 Pa were impregnated with different liquids by simple immersing them in that liquid for at least 24 hours.

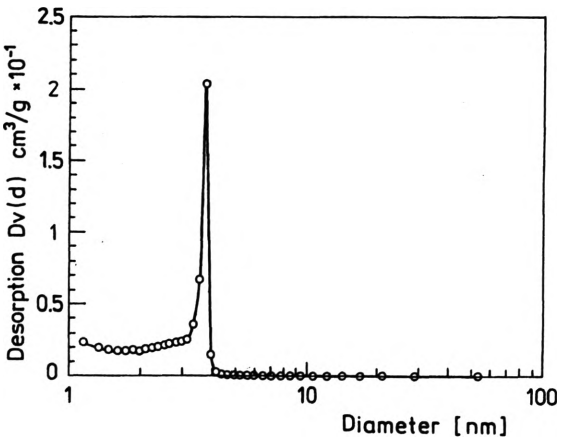

Fig. 1. Pore size distribution of one of the sol-gel glasses used in this study

2.2. Diffusion measurements

To measure diffusion coefficient we used radioactive tracer method, diaphragm cell, and light absorption. Each technique is discussed separately below.

Tracer diffusion

Tracer diffusion measurements were limited only to water and cyclohexane. Experiments were performed on long cylindrical samples. Presoaked porous glass was placed in a vertical orientation into a flask. To prevent evaporation of the solvent during the experiment, the side surface of the cylindrical sample was sealed with a thin layer of TorrSeal. On the top surface of the cylindrical sample a small

amount of radioactive liquid, 37 kBq, was placed. The flask was sealed and immediately stored in a thermostat bath at a temperature of 301 $\pm$0.5 K. To satisfy the semi-infinite boundary condition, the diffusion of the tracer through the pores was stopped after about 24 hours. During that time tracer molecules diffused through about one half of the length of the sample, and we were able to ignore the reflections at the other end.

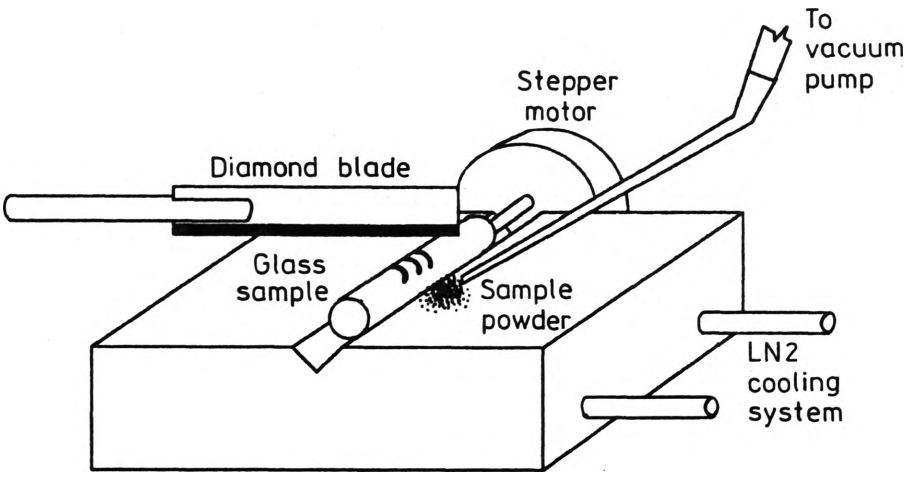

Fig. 2. Diamond saw operating at low temperature, below the freezing point of the solvent used to section the glass

A diamond saw shown in Figure 2 was designed to section the samples at about 2 mm intervals. Porous glass samples were removed from the thermostat and to prevent evaporation and to eliminate the diffusion during the sectioning of the sample, the samples were rapidly cooled down to 268 K, to freeze the solvent. The saw was also operating at the same temperature. The relative orientation of the sample and the blade remained unchanged during the sectioning. The cuts were parallel to the top surface of the sample. The diamond blades, 0.8 mm thick, made 3 mm deep grooves in the samples, and using a vacuum system we collected the powder produced by the blade directly into preweighed vials filled with a toluene based scintillation solution. The mass of the powder was obtained by reweighing the vials. Scintillation measurements were conducted on a Beckman Liquid Scintillation System at various times after the powder has been collected into the vials. To promote the mixing of the scintillation solution with the powder, the vials were placed on a shaker.

Diaphragm cell

The diffusion coefficients of acetone, acetonitrile, toluene, chloroform, and cyclohexane were measured using the diaphragm cell illustrated in Fig. 3. This is a simple and very accurate method for studying isothermal diffusion for binary solvents. When the pure solvent is placed in the top compartment and the binary solution in the bottom compartment of the cell, the diffusion coefficient through

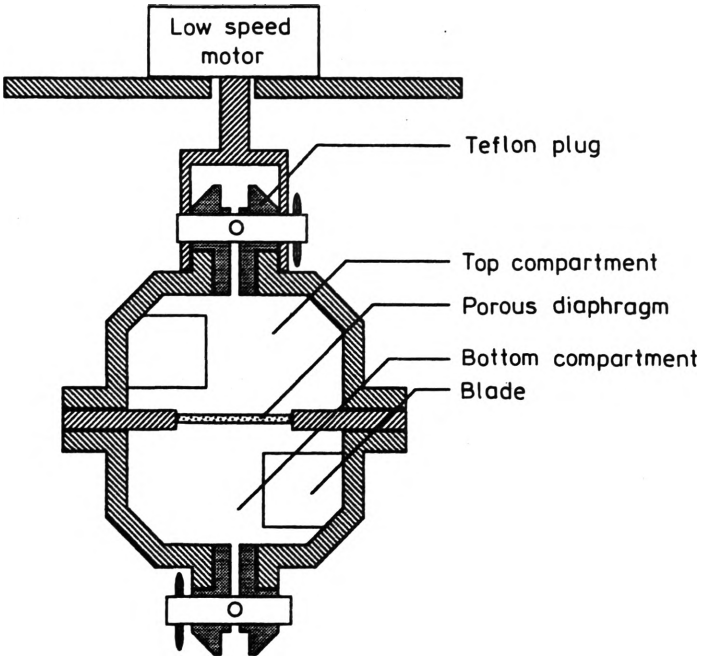

Fig. 3. Diaphragm cell used for the diffusion studies. During the measurements the cell was immersed in water bath of controlled temperature. Porous silica membrane was glued to stainless steel body of the cell by TorrSeal, a very low vapour pressure glue

a porous diaphragm separating the two compartments can be found from [20]

$$D\beta t = \lambda \ln\{(C_1^0 - C_2^0)/(C_1 - C_2)\} \tag{5}$$

where: λ – constant that depends on the volume of the cell and the volume of the diaphragm, t – duration of the experiment, C_1^0 and C_2^0 – initial concentrations in the bottom and in the top compartments, respectively, C_1 and C_2 – final concentrations at the end of the experiment, β – cell constant dependent on the porosity of the membrane.

To be able to use Equation (5), before the measurements, a concentration gradient of deuterated solvent inside the sol-gel diaphragm was established. Next, a 15% solution of deuterated solvent was placed in the bottom compartment. In the top compartment of the cell we place pure solvent. In the diaphragm method, it is critical to secure uniform concentration of solutions in both cells. This was accomplished by spinning the cell by a low speed motor. The rotational motion of the cell caused the blades mounted inside the compartments to stir the solution. The motor rotated clockwise for one minute, stopped, rotated counterclockwise for one minute and stopped again. These acceleration-deceleration cycles mixed the liquids and the diffusive boundary layers near the diaphragm were eliminated [21]. The cell was placed into a thermostat at $T = 28°\,C$ or $21°\,C$. A typical experiment lasted from 2 to 10 days. At the end of this period several millilitres of solutions were removed from both compartments and IR absorption spectra were recorded. Using

Lambert–Beer law, we determined the concentrations of deuterated solvents and next calculated $D\beta$. Concentration of acetone was found from intensities of the 2255 cm^{-1} band, for chloroform from the C-D stretch centered at 2253 cm^{-1}, for cyclohexane we used the C-D stretch at 2193 cm^{-1}, for acetonitrile the 835 cm^{-1} band, and for toluene the 544 cm^{-1} band.

2.3. Diffusion of metal cations

The diaphragm cell is not recommended to study diffusion of ionic solutions [20]. Therefore, a different procedure was employed. Sol-gel samples in the form of parallelepiped had five of their six faces sealed using transparent silicone sealant and were next sandwiched between microscope slides. Only one face remained exposed to the liquid. At various time intervals the sample was removed from the solution and the concentration of metal cations at various locations within the sol-gel samples was measured using visible absorption spectroscopy. Efforts were made to reduce the time the samples were removed from the solution, typically it took less than 2 minutes to record a spectrum. After the spectra had been recorded, the sample was immediately returned to the solution. Absorption spectra were recorded on a Cary 13 spectrometer.

3. Results

The application of a very thin layer of radioactive liquid to a long cylindrical porous glass of 6 cm in length resulted in the maximum penetration of about 3 cm in 24 hours. These experimental conditions can be approximated by the diffusion in a semi-infinite medium. The activity C of radiotracers at a distance x from the top of the semi-infinite sample can be found by solving the Fick second law [22]

$$C = \frac{M}{(\pi D t)^{1/2}} \exp\left(-\frac{x^2}{4Dt}\right) \tag{6}$$

where: M – total activity of labelled molecules, D – diffusion coefficient, and t – diffusion time. Taking logarithm of both sides of Eq. (6), we get a linear relation between $\ln C$ and x^2. In each experiment the plots of $\ln C$ *versus* x^2 were linear, an example is shown in Fig. 4. The average diffusion coefficient was found from 12 independent runs, and at 301 K for water it was 1.8×10^{-10} m^2/s, while for cyclohexane it was 1.0×10^{-10} m^2/s. Although uncertainty in determining self-diffusion coefficients in individual runs was relatively small, about $\pm 2\%$, the reproducibility was poor, 10% for water and 18% for cyclohexane.

A simple comparison between the average values obtained for cyclohexane by using the diaphragm cell ($D\beta = 6.28 \times 10^{-7}$ s^{-1}) and from the radioactive tracer diffusion study ($D = 1.0 \times 10^{-10}$ m^2/s) allowed us to determine that $\beta = 6820$ m^{-2}. This value was used to calculate the diffusion coefficients for other liquids using the diaphragm cell. The results are listed in the Table. Each value is an average of 5 (chloroform) to 10 (acetone, acetonitrile, toluene, cyclohexane) measurements. The precision of $D\beta$ measurements was very good, usually better than $\pm$ 4%, but taking

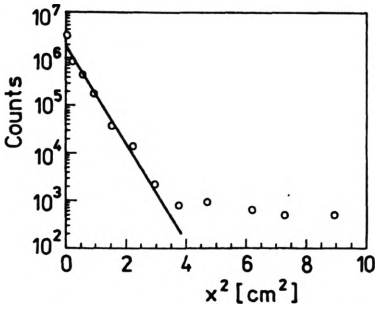

Fig. 4. Specific activity against x^2 for $C_6H_{11}{}^3H$ tracer in cyclohexane, C_6H_{12}, in porous sol-gel glass. The slope gives the diffusion coefficient D

into account the accumulated error in determining β we estimate that the absolute values in the Table are accurate only within 20%. However, the data in the Table provide very accurate data on relative changes in the D values for various solvents.

Table. Diffusion coefficients inside porous silica for different liquids [$\times 10^{-10}$ m^2/s]

Tracer diffusion	Diaphragm cell	$T = 21°$ C; pore size 2.9 nm	$T = 28°$ C; pore size 2.9 nm	$T = 28°$ C; pore size 2.9 nm
water				1.8
cyclohexane				1.0
	cyclohexane	0.74	1.0	
	toluene	0.9		
	chloroform	1.5		
	acetonitrile	4.0		
	acetone	5.6		

For the bulk water $D = 2.2 \times 10^{-9}$ m^2/s [20]. Comparison of the data in the Table indicates that the motion of water in porous media is hindered, in porous glass it is 12 times slower than in the pure liquid. Similar results were obtained for cyclohexane. Translational motion of cyclohexane molecules in small pores is 14 times slower than in the pure phase. (Diffusion coefficient of cyclohexane in the bulk system is $D = 1.44 \times 10^{-9}$ m^2/s). This is a typical result and has been observed previously for many liquids [17], [25].

Recently [23], [24], we completed computer simulations for cyclohexane inside a model cylindrical pore of diameter 2.8 nm, and the calculated value of the diffusion coefficient was 5.82×10^{-10} m^2/s. The discrepancy between the experimental results and computer simulations can be attributed to the differences in the pore structures of the modelled system and the real sol-gel glass. The model assumed a cylindrical shape of the pore. Of course, the pores in the sol-gel have different diameters. Although our samples have narrow pore size distribution, it is clearly asymmetric, compare Fig. 1. About 90% of the pores had diameters between 2.0 and 3.1 nm with the average value of 2.9 nm, but the total volume of the pores with diameters less

than the average diameter was greater than that of the larger pores. Small pores limit the diffusion rate to a greater extent than larger pores. To improve accuracy of numerical model, one could simulate molecular motion in pores of various diameters and next using the pore size distribution function find the average diffusion coefficient [25]. For obvious time limitation we did not run such simulations. Another effect to be considered is the pore connectivity and effective path length of the diffusing species inside the sample. In addition, physical traps ("dead end" cavities) may further slow down the transport of the solvent through the porous medium. It is common to use the tortuosity factor to account for the differences between the diffusion coefficient in a cylindrical cavity and through the actual system of interconnected pores [25], [26]. By comparing computer simulation and experimental data we estimate that the tortuosity factor for the sol-gel glass used in this study is 5.8.

Even a brief analysis of the data in the Table indicates that molecular motion for different liquids inside small pores is hindered to different degrees. It is seen that liquids that have large dipole moments, such as acetone or acetonitrile, move faster than a neutral solvent such as cyclohexane. This is a surprising result. Although the diffusion coefficients for those solvents in the unbound system (4.8, 4.05×10^{-9} m^2/s for acetone and acetonitrile, respectively) are greater than that for cyclohexane, their translational displacement inside the pores is hindered to a lesser extent than cyclohexane. Strong hydrogen bonding between water or acetone and hydroxyl groups on the silica surface was expected to immobilize adsorbed molecules and thus slow down their translational displacement. In addition, polar liquids form a double layer near the pore walls which is expected to further slow down molecular motion by effectively reducing the pore diameter. The double layer structure for surface molecules has been observed before for pyridine and acetonitrile [17], [27]. Molecules in the first layer are all oriented with respect to the surface resulting in strong repulsive forces between parallel (or almost parallel) dipole moments. To stabilize this structure, the second layer must be formed with the molecules oriented antiparallel. Nonpolar liquids, such as cyclohexane and molecules possessing small dipole moments, toluene (diffusion coefficient in the bulk phase $D = 2.27 \times 10^{-9}$ m^2/s) and chloroform (D in the bulk phase 3.3×10^{-9} m^2/s) form only a single layer near the pore walls. Since there is no hydrogen bonding between cyclohexane or toluene and silica surface, and very weak interaction between chloroform and silanols, those molecules were expected to move faster than highly polar molecules such as acetone and acetonitrile. At the present time, no explanation for the observed diffusion coefficients has been proposed.

Water and acetone were used to dissolve neodymium nitrate. Although solubility of the salt in water is better than in acetone, all attempts to produce a permanent concentration gradient in the porous sol-gel glass using water as the solvent failed. In the initial stages of the impregnation process, Nd^{3+} cations diffused into the pores and a concentration gradient was clearly observed even with a naked eye. However, the cations were not immobilized inside the pores, and were able to move inside the glass. During evaporation of water, the motion of cations was so pronounced that

after the drying process was completed the dopant material was almost uniformly distributed throughout the sample. To avoid this problem, we considered using organic solvents. The best results were obtained for acetone. It was easy to obtain the concentration gradient, and as we will discuss later, the gradient remained unchanged after the solvent was removed from the pores.

Assuming that the sol-gel sample can be treated as a semi-infinite medium, and the diffusion is uniform along the x-axis, the diffusion coefficient for metal cations can be determined by solving Fick's law [22]. Because the sample was immersed in a large volume of the solution and the solution was constantly being stirred, we were able to assume that during the diffusion process the concentration of the cations at the boundary remained constant. The sample can be considered semi-infinite if the diffusing elements reach a depth which is a fraction of the total length of the sample, and, consequently, there is no need to consider reflections at the opposite end. When the diffusion process started there was no neodymium inside the sol-gel glass. For these conditions, the concentration of neodymium inside the sample at a distance x from the open surface is given by [22]

$$C = C_0 \operatorname{erfc}[x/2(Dt)^{1/2}] \tag{7}$$

where t is the elapsed time, and D is the diffusion coefficient. The error function complement, erfc, is defined as

$$\operatorname{erfc} z = \frac{2}{\sqrt{\pi}} \int_z^\infty \exp(-y^2)dy. \tag{8}$$

The concentration of neodymium at various depths inside the sample was determined using Lambert–Beer law from the absorption spectra. From Figure 5 it is seen that the intensity of the 740 nm peak diminishes as the probing beam is moved inward from the edge of the sample.

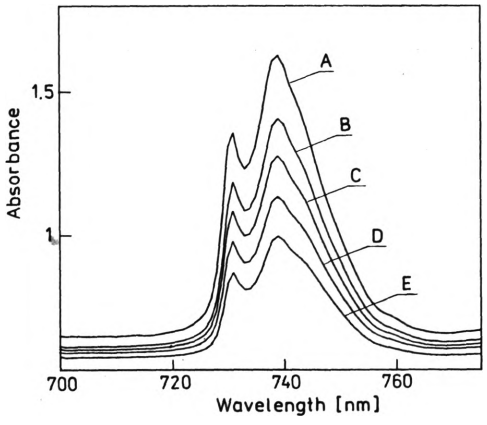

Fig. 5. Absorption spectra recorded by scanning a sample along the axis of one-dimensional diffusion. Postion of the beam: A – 2 mm from the sample edge, B – 2.6 mm, C – 3.3 mm, and D – 4.6 mm. Diffusion time – 6 hours. Solvent – water

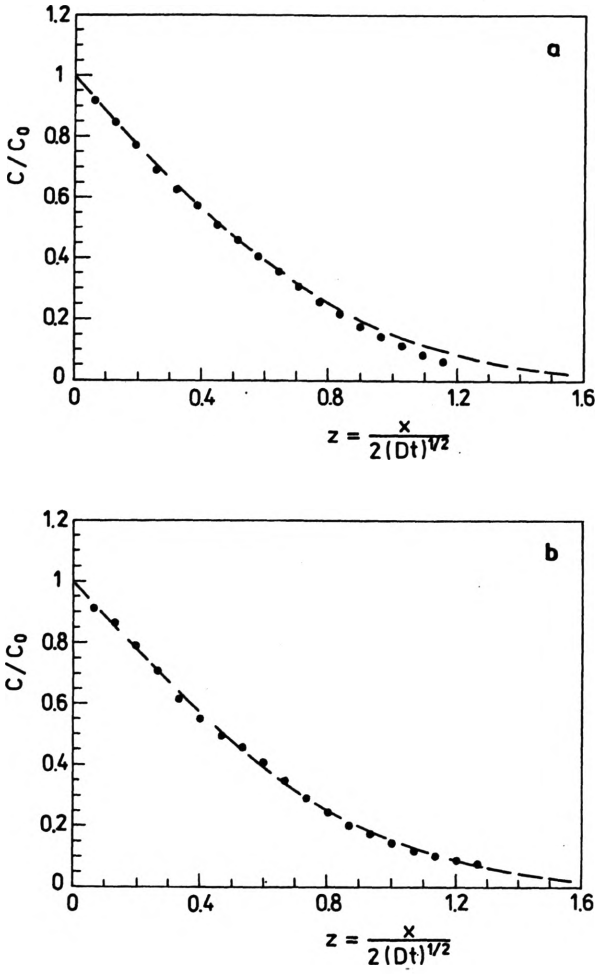

Fig. 6. Comparison of experimental data on concentration of neodymium, solid symbols, with theoretical predictions, Eq. (7), broken lines. **a** — solvent water, pore diameter 2.9 nm, the best fitting obtained for the diffusion coefficient $D = 2.1 \times 10^{-10}$ m²/s; **b** — solvent acetone, average pore diameter 2.9 nm, $D = 6.5 \times 10^{-11}$ m²/s

For the aqueous solutions a comparison of experimental results with the theoretical model was never fully satisfactory. As illustrated in Fig. 6a, a relatively good agreement between the experimental data and theoretical predictions was obtained for concentrations measured for small penetration depths, but rather poor agreement was observed for larger x values. And *vice versa*, a good fit for large depths meant a poor agreement for small x values. This observation can be explained in terms of the dependence of the diffusion coefficient on the salt concentration. There is experimental evidence that in aqueous unbounded solutions of metal salts, the diffusion coefficient of the cations may decrease by a factor of two when the concentration of the salt is increased to about 2 mol/l [20]. During the impregnation process, the concentration of neodymium cations inside the porous glass changes in

time and is a function of the distance from the surface. This means that it is impossible to use Eq. (7) to determine D, but only estimate its lower and upper limits. For aqueous solution we estimate that D varies between 2.2×10^{-10} m/s and 1.3×10^{-10} m^2/s.

For acetone solutions the agreements between the experimental data and Eq. (7) were much better and, as illustrated in Fig. 6b, it was possible to reproduce almost entire concentration profile by the theoretical function. Contrary to the aqueous solutions, the discrepancies for large values of x were small and it was possible to evaluate the diffusion coefficient. For the 2.9 nm pores the diffusion coefficient for neodymium is 6.5×10^{-11} m^2/s $\pm 0.5 \times 10^{-11}$ m^2/s, whereas for larger pores of diameter 3.7 nm it is 11.3×10^{-11} m^2/s $\pm 0.7 \times 10^{-11}$ m^2/s. These results are average of four independent experiments, in each we used different samples from the same batch of monolithic sol-gel glass sample.

The data on D was useful to approximate the time of diffusion to obtain concentration gradients depicted in Fig. 7. In this experiment neodymium solution

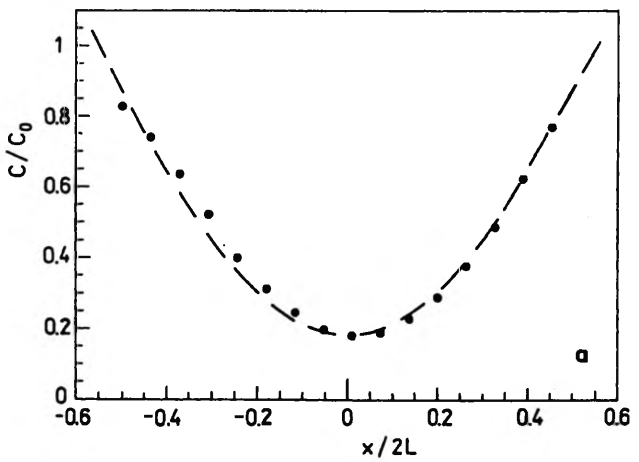

Fig. 7a

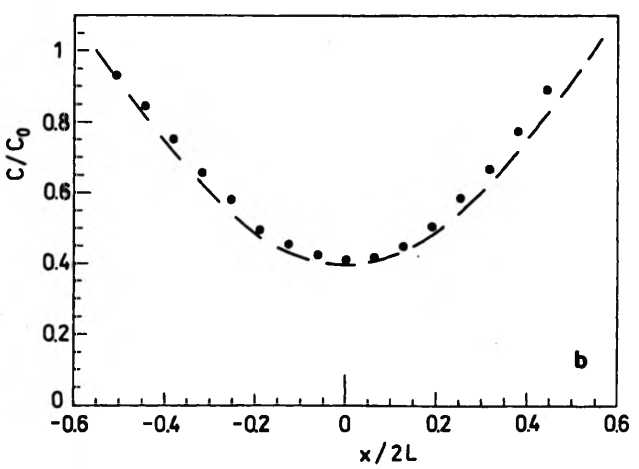

Fig. 7b

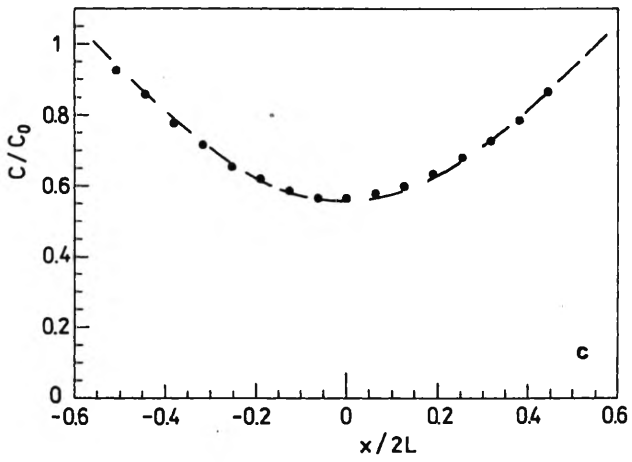

Fig. 7c

Fig. 7. Solid symbols – experimental data for diffusion of neodymium cations inside a parallelepiped sample along the x-axis from opposite sides. Broken line – theoretical predictions from Eq. (9) assuming $D = 2.1 \times 10^{-10}\,m^2/s$. a – results for the diffusion time $t = 6$ hours, b – for $t = 9$ hours, and c – for $t = 12$ hours. The length of the sample $2L = 22$ mm. Solvent – water

was allowed to flow into the porous material through two opposite faces of a long parellelepiped. After a predetermined time we measured the concentration of the dopant inside the sample along the x-axis. These data were compared with the theoretical model for diffusion in a plane sheet with the surfaces at $x = L$ and $x = -L$ kept at uniform concentration C_0. Since at the start of the experiment the initial concentration within the sample was zero, the concentration inside the sample can be expressed as [22]

$$\frac{C(x)}{C_0} = 1 - \frac{4}{\pi} \sum_{n=0}^{\infty} \frac{(-1)^n}{2n+1} \exp\left[-\frac{D(2n+1)^2\pi^2 t}{4L^2}\right] \cos\left[\frac{(2n+1)\pi x}{2L}\right]. \tag{9}$$

As seen in Figure 7, the agreement between the experimental data and Equation (9) is satisfactory. It is interesting to note that the profiles shown in Fig. 7 are almost parabolic and, as indicated by Eq. (1), the doped glass could be used as a GRIN lens.

Once we determined the diffusion coefficient we attempted to make a flat lens by diffusing Nd^{3+} into a sol-gel glass in the form of a cylinder of diameter $a = 15.5$ mm. The two parallel faces of the cylinder were sealed and neodymium diffused radially into the porous samples presoaked with acetone. Assuming that the salt concentration in the solution on the outside of the sample C_0 is constant and does not vary in time, the concentration C inside the sample is then a function of radius and time, and according to CRANK [22] it is given by

$$\frac{C(r)}{C_0} = 1 - \frac{2}{a} \sum_{n=1}^{\infty} \exp(-Dt\alpha_n^2) \frac{J_0(r\alpha_n)}{J_1(a\alpha_n)} \tag{10}$$

where J_0 and J_1 are the Bessel functions of the first kind, and α_n are the roots of the Bessel function of the first kind of zero order

$$J_0(a\alpha_n) = 0. \tag{11}$$

We used Equation (10) to predict various concentration profiles for samples of average pore diameter 2.9 nm. The geometry of the beam within the Cary 13 spectrometer (rectangular cross-section) precluded precise Nd concentration measurements as a function of the distance from the centre of the disk. Instead we measured the focal lengths of the produced flat lenses. When the exposure time was set to 30 hours, a 6 cm focal length lens was produced.

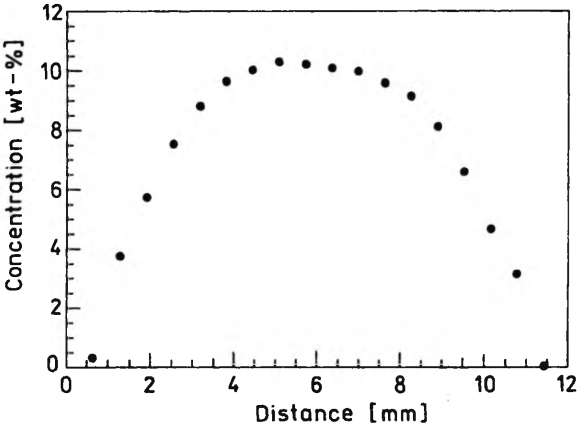

Fig. 8. Example of the reverse concentration gradient obtained by immersing impregnated sample into acetone

Outward concentration gradients of metals within sol-gels were made by uniformly loading samples with neodymium by soaking a gel for 48 hours in a solution. The samples were next dried, sealed and then placed in pure solvent for a specific amount of time. The leaching of the neodymium from the sample resulted in the concentration gradient, an example is shown in Fig. 8.

As seen from the data in the Table, the translational motion of water inside the pores is about 12 times slower than in the bulk liquid. This result is similar to that obtained for other liquids in small pores [28]. What is surprising is that the diffusion coefficient of neodymium cations in the pores of the same size is about the same as that of the solvent, water. Water molecules adsorb on the pore walls and form a double layer which effectively reduces the pore diameter. It was expected that the motion of neodymium cation and its coordination sphere of estimated diameter of about 1 nm will be highly restricted and that the diffusion coefficient will be much smaller. It is possible that the cation and its coordination sphere do not diffuse together as a one unit. Instead, water molecules may be replaced by others when the cation moves along the pore. This model may explain relatively fast motion of Nd^{3+} cations in porous glass.

The measured mobility of acetone molecules in the pores of diameter 2.9 nm is surprisingly fast ($D = 4.3 \times 10^{-9}$ m^2/s), about twice as fast as of water molecules.

But the diffusion of neodymium in acetone filled pores is much slower, $D = 6.5 \times 10^{-11}$ m^2/s. At the present time, no mechanism explaining these results has been proposed, but the large difference between diffusion coefficients for acetone and Nd^{3+} explains why it is relatively easy to remove the solvent from the pores without altering the concentration profile of the neodymium in porous sol-gel glass. Comparing the diffusion coefficient data for Nd^{3+} in the pores various sizes, it is noticed that in the pores of larger diameters the motion of the cations is less restricted and neodymium can move faster.

In this investigation we measured transport mechanism through a macroscopic porous material, and not through a single small pore. This means that although the average pore diameter remained the same, variations in sample pore connectivity, porosity, local density, and other parameters may drastically alter the value of the diffusion coefficient measured for samples obtained under different conditions. To avoid this problem almost all experiments were conducted on a set of samples obtained from one batch, and when different batches were used, we made sure that they were prepared under identical conditions. In addition, adjustment of the pH of the solvent [20] or modification of the surface groups may further change the diffusion coefficient. Therefore, the values of D reported in this paper are specific only for the material used in this study, but we believe that the conclusions are general, and independent of the manufacturing procedure.

Loading of stable glass monoliths allowed us to obtain large concentrations of metal cations in the pores. For a sample of the total pore volume 0.5 cm^3/g and average pore diameter 2.9 nm it was possible to increase the concentration of neodymium to 20% of the original weight of the sample. Of course, such loading may result in phase separation, and for practical applications it may be desired to work with smaller amounts of the dopant material inside the pores [29]. For a sample in which the concentration of neodymium was less than 5% of the original dry mass of the porous matrix we recorded fluorescence spectra in the near infrared region. Prior to the measurement the sample was fired at 1000° C. The peak at 1.06 μm due to the $^4F_{3/2} - {}^4I_{11/2}$ transition was very sharp which indicated that the extent of the phase separation although possible was very small.

Absorption spectra of neodymium salt dissolved in water and acetone are slightly different. As seen from Figures 9 and 10, absrption spectra have different relative intensities and contours in water and in acetone based solutions. The relationship between the coordination sphere of the neodymium +3 ion and the intensities and band shapes of the $f-f$ bands is complex and not quantitatively understood [30]. But it is obvious that acetone plays an important role in the coordination sphere. The structure and stability of the coordination sphere is probably the factor limiting the diffusion of neodymium inside the pores. It is interesting to note that the absorption spectra of acetone solutions of neodymium nitrate in an unbound system and inside the pores are practically identical (compare Fig. 10). As seen from Figure 9, the same is true for the sol-gel glass impregnated with neodymium nitrate dissolved in water; spectra of the water solution and of the impregnated samples are very similar. This means that the structures of

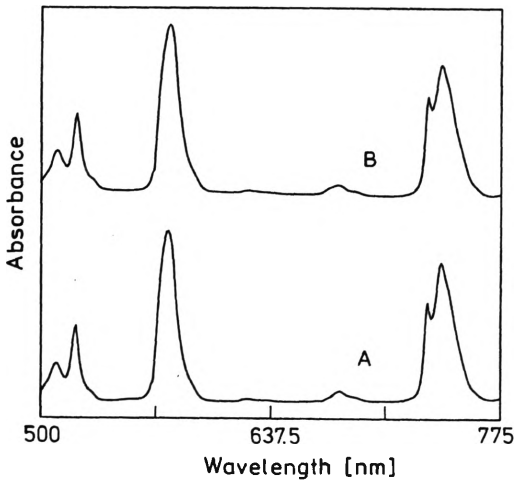

Fig. 9. Absorption spectra of 2.2 M water solution of neodymium nitrate in the unbound system (A) and inside the porous sol-gel glass (B)

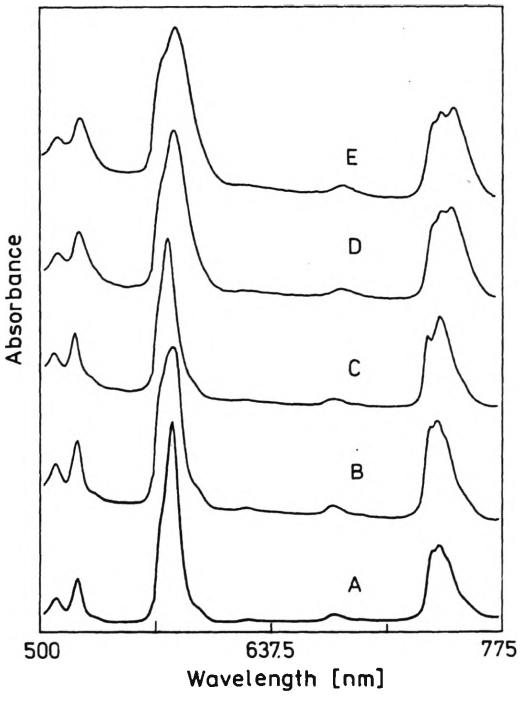

Fig. 10. Absorption spectra of acetone solution of neodymium nitrate in the unbound system (A); in the porous sol-gel glass (B); the same sample after being dried (C); fired to 500° C (D); and 800° C (E)

neodymium complexes do not change when they move from the bulk system into the pores.

After the samples were dried significant changes in the spectra of Nd^{3+} were observed, as displayed in Fig. 10. Since the drying was carried under normal conditions at roon atmosphere, acetone molecules near Nd^{3+} cations were replaced with water molecules adsorbed from the atmosphere and absorption spectra of dried samples became similar to the spectra of water based systems (compare spectra A in Fig. 9 and A in Fig. 10). After acetone in the cordination sphere was replaced by water further temperature treatment of the samples was similar to that of samples impregnated with water solutions. When temperature was increased above 300° C significant band shifts and broadening were observed. These facts indicate that Nd^{3+} sites have relatively high symmetry with very similar crystal fields in wet gels. The Nd^{3+} ions do not seem to enter the silica network during the impregnation process and remain coordinated to solvent molecules. Interactions with surface groups, such as O−H and O−R groups, become important at higher temperatures when Nd^{3+} ions progressively lose their coordination bonds with water and solvent. These molecules are partially substituted by the hydroxyl and methoxy groups on the silica surface, as may be deduced from the changes in the spectra shown in Fig. 10. Further increase in temperature results in pore closure and the peaks are further shifted and broadened. When hydroxyl and methoxy groups are removed from the sample, the Nd^{3+} sites are surrounded by silica. The local field generated by silica is highly inhomogeneous and varies from site to site resulting in broad bands.

We have not studied the diffusion of anion, NO_3^-, because after drying and firing to 500° C these species were not found in the sample. They probably escaped from the gel in the form of HNO_3.

As stated before, stable concentration gradients were obtained only for acetone solutions. The concentration profiles of cations inside the sample were unchanged as the temperature was increased up to 1000° C.

4. Conclusions

Diffusion coefficients of water and cyclohexane in porous sol-gel glass of average pore diameter 2.9 nm were obtained using a radioactive tracer technique. This information was applied to calibrate the membrane in the diaphragm cell which was subsequently used to measure the diffusion coefficient for cyclohexane, acetone, toluene, acetonitrile, and chloroform. Translational motion of polar liquids inside the pores was found to be faster than that of neutral, not wetting solvents.

In this study we showed that it is possible to produce both diverging and converging lenses by doping porous sol-gel glass with metal cations. Instead of aqueous solutions it is recommended to use organic solvents in which the diffusion of the dopant material is slower than that of the solvent. After acetone is evaporated from the pores, it is replaced by atmospheric water. When water is removed from the pores, Nd cations are incorporated into the glass framework.

Metal ion coordination sphere in porous sol-gel glass is primarily affected by solvent interactions, and to a lesser extent depends on the structure of the pores.

The concentration of the dopant material can be controlled by adjusting the concentration of the liquid outside of the glass. The rate of penetration at any given concentration is proportional to the square root of time, and the time for any point inside the sol-gel glass to reach a given concentration is proportional to the square of its distance from the surface and varies inversely as the diffusion coefficient. Large concentration of the dopant material, exceeding 10% of the total mass, may be easily introduced into the glass. Samples of large diameters, in excess of 15 mm, can be easily doped with index modifying metal. Concentration gradients are maintained in densified sol-gel glass.

Acknowledgements – Acknowledgement is made to the donors of the Petroleum Research Fund administered by the American Chemical Society. This study was also supported by a TCU Research Fund.

References

[1] YAMAGUCHI T., FUJII K., KITANO I., J. Non-Cryst. Solids **47** (1982), 283.
[2] OHMI S., SAKAI H., ASAHARA Y., YONEDA Y., IZUMITANI T., Appl. Opt. **27** (1988), 496.
[3] YAMANE M., [In] *Ultrastructure Processing of Advanced Materials*, [Eds.] R. D. Ulhmann, D. R. Ulrih, Wiley, New York 1992.
[4] YAMANE M., CALDWELL J. B., MOORE D. T., [In] *Better Ceramics Through Chemistry*, Vol. 2, [Eds.] C. J. Brinker, D. E. Clark, North-Holland, Amsterdam 1986.
[5] KONISHI S., SHINGYOUCHI K., MAKISHIMA A., J. Non-Cryst. Solids **100** (1988), 511.
[6] HENCH L. L, LA TORRE G. T., DONOVAN S., MAROTTA J., VALLIERE E., SPIE, *Sol-Gel Optics II*, 1992, KUNETZ J. M., HENCH L. L., [In] *Chemical Processing of Advanced Materials*, [Eds.] L. L. Hench, J. West, New York 1992.
[7] WEST J., HENCH L. L., Chem. Rev. **90** (1990), 73.
[8] ZERDA T. W., VASCONCELOS W. L., HENCH L. L., J. Non-Cryst. Solids **121** (1990), 143.
[9] VASCONCELOS W. L., Ph. D. dissertation, University of Florida, 1989.
[10] CHE T., CARNEY R. V., KHANARIAN G., KEOSIAN R. A., BORZO M., J. Non-Cryst. Solids **102** (1988), 280.
[11] AVNIR D., LEVY D., REISFELD R., J. Phys. Chem. **88** (1984), 5956.
[12] GVISHI R., REISFELD R., J. Non-Cryst. Solids **128** (1991), 69.
[13] KUSELMAN I., LEV O., Talanta **40** (1993), 749.
[14] WU S., ELLERBY L. M., COHAN J. S., DUNN B., EL-SAYED M. A., VALENTINE J. S., ZINK J. I., Chem. Mat. **5** (1993), 165.
[15] LEVY D., SERNA C. J., OTON J. M., Mat. Lett. **10** (1991), 470.
[16] AEGERTER M. A., JAFELICCI M., SOUZA D. F., ZANOTTO E. D., *Sol-Gel Science and Technology*, World Scientific, Singapore 1990.
[17] ZERDA T. W., HOANG G. C., Chem. Mat. **2** (1990), 372.
[18] NIKIEL L., ZERDA T. W., J. Phys. Chem. **95** (1991), 4063.
[19] ZERDA T., [In] *Chemical Processing of Advanced Materials*, [Eds.] L. L. Hench, J. West, Wiley, New York 1992.
[20] TYRRELL H. J. V., HARRIS K. R., *Diffusion in Liquids*, Butterworths, London 1984.
[21] ZERDA T. W., BRODKA A., COFFER J., J. Non-Cryst. Solids **168** (1994), 33.
[22] CRANK J., *The Mathematics of Diffusion*, Clarendon Press, Oxford 1986.
[23] BRODKA A., ZERDA T. W., J. Chem. Phys. **97** (1992), 5676.
[24] ZERDA T. W., BRODKA A., *NATO ASI on High Pressure Chemistry, Biochemistry and Materials Science*, [Eds.] R. Winter, J. Jonas, Kluwer, Amsterdam 1993.
[25] SAHIMI M., J. Chem. Phys. **96** (1992), 4718.
[26] SHAO Y., KOONE N., ZERDA T. W., *Better Ceramics Through Chemistry*, Vol. 7, submitted.

[27] WATSON J., ZERDA T. W., Appl. Spectrosc. **45** (1991), 1360.
[28] KLAFTER J., DRAKE J. M., [In] *Molecular Dynamics in Restricted Geometries*, Wiley, New York 1989.
[29] MACKENZIE D., private communication.
[30] STEPHENS E. M., SCHONE K., RICHARDSON F. S., Inorg. Chem. **23** (1984), 1641.

Received June 6, 1994